

Nanodiamond-Polymer Composite Fibers and Coatings

Kristopher D. Behler,[†] Antonella Stravato,^{†,§} Vadym Mochalin,[†] Guzeliya Korneva,^{†,*} Gleb Yushin,^{†,‡} and Yury Gogotsi^{†,*}

[†]A.J. Drexel Nanotechnology Institute and Department of Materials Science and Engineering, [‡]A.J. Drexel Nanotechnology Institute, and Department of Chemistry, Drexel University, 3141 Chestnut Street, Philadelphia, Pennsylvania 19104. [§]Current address: Department of Industrial and Mechanical Engineering, University of Roma Tre, 00146 Rome, Italy. [‡]Current address: Georgia Institute of Technology, School of Materials Science and Engineering, Atlanta, Georgia 30332.

Nanodiamond (ND) powder, also known as ultradispersed diamond (UDD), exhibits unique properties of diamond on the nanoscale and is becoming one of the more widely studied nanomaterials.^{1–6} Superior hardness and thermal conductivity of the diamond core is combined in nanodiamond powders with large accessible surface area covered by readily tailorable surface functional groups.^{1,7,8} The wide band gap of the diamond (~5 eV) renders it highly absorptive toward UV light, but transparent in the visible and IR range.¹ ND is produced by a detonation synthesis in large volumes and is a relatively inexpensive carbon nanomaterial for a broad range of potential applications, including composites.^{9–11} As a powder, ND could be introduced into fibers, coatings, or other shapes to harness its useful properties. One major obstacle for ND composites is the ability to deliver nanodiamond in the form of well-dispersed particles¹² into a polymer matrix. Traditional polymer processing techniques such as casting and extrusion have yielded poor dispersion due to agglomeration/reagglomeration of the nanodiamonds within the polymer matrix leading to a compromise of the properties.¹³ Also, the addition of more than several percent of nanodiamond to the whole volume of a polymer component would substantially increase the cost and weight. Therefore, diamond should preferably be used in those places where it is needed, for example as a surface coating.

Electrospinning provides many benefits stemming from the small and tunable fiber diameter. Polymer composites produced *via* the electrospinning method allow for a polymer nanofiber to act as a host for nanoparticles.^{14–22} Polymer nanofibers can be used as a coating or appliqués,^{23,24} thus

ABSTRACT While nanocrystalline diamond is quickly becoming one of the most widely studied nanomaterials, achieving a large fraction of diamond nanoparticles in a polymer coating has been an unresolved problem. In this work, polymer nano- and microfibers containing high loadings of 5 nm diamond particles (up to 80 wt % in polyacrylonitrile and 40% in polyamide 11) have been demonstrated using electrospun nanofibers as a delivery vehicle. The electrospun nanofibers with a high load of nanodiamond in the polymers were fused into thin transparent films, which had high mechanical properties; an improvement of 4 times for the Young's modulus and 2 times for the hardness was observed already at 20% nanodiamond in polyamide 11. These films can provide UV protection and scratch resistance to a variety of surfaces, especially in applications where a combination of mechanical, thermal, and dielectric properties is required.

KEYWORDS: nanodiamond · polymer · nanofibers · electrospinning · composite materials · thin films · coatings

delivering nanodispersed particles while effectively preventing their agglomeration. The confinement of the fiber diameter, polymer surface tension, and strong electrostatic force pulling the fiber in the electrospinning process may help in deagglomeration of nanoparticles, similarly as it has led to a debundling of single-walled carbon nanotubes and their alignment along the fiber axis.¹⁵ In addition, as soon as the fiber solidifies upon evaporation of the solvent during electrospinning, reagglomeration of nanoparticles is effectively suppressed; thus, a resulting nanocomposite incorporates uniformly dispersed, size-confined nanoparticles.

So far, various nanomaterials have been incorporated into electrospun fibers. Among them are ceramic nanoparticles,^{17,18,21} nanowires,¹⁴ quantum dots,^{19,22} nanotubes,^{15,20} and others. While there have been more than a hundred of articles published on electrospun polymer-nanotube fibers in the past 5 years, there are no reports on electrospun ND-polymer fibers. At the same time, ND powders, being biocompatible^{1,25–27} and having a

*Address correspondence to gogotsi@drexel.edu.

Received for review July 15, 2008 and accepted January 27, 2009.

Published online February 4, 2009.
10.1021/nn800445z CCC: \$40.75

© 2009 American Chemical Society

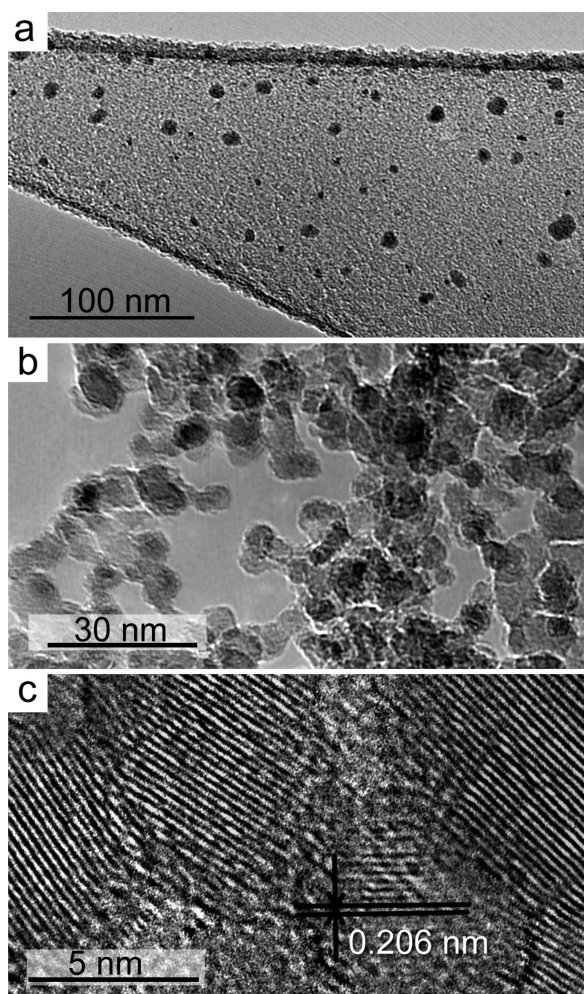


Figure 1. Low resolution TEM of oxidized ND powder containing both the individual particles (a) and loosely bound agglomerates (b). High resolution TEM (c) showing mostly pristine nanodiamond particles with little content of disordered carbon.

tailorable and easily accessible surface, certainly have a great potential to be used as a filler of a polymer matrix in many applications. By harnessing electrospinning as a procedure to produce and apply thin films to various substrates,²⁴ ND-polymer composites could be transformed into thin scratch-resistant coatings that would effectively protect from UV rays on windows, or prevent degradation of UV sensitive materials. Diamond-containing electrospun fibers could be used in smart and UV-protecting clothing, for biomedical applications such as wound dressings,^{28,29} cell growth scaffolds,^{30,31} sensing,³² and drug delivery systems.^{33–36} ND modification and functionalization opens up new avenues for ND applications in which electrospun ND-polymer composites can be utilized. As an example, fluorescent nanodiamond can be embedded into a polymer matrix and used for applications such as medical diagnostics, imaging and labeling,^{37,38} as well as photovoltaics.

The objective of this work was to demonstrate feasibility of manufacturing composite polymer-nanodiamond fibers by electrospinning. Moreover, we will

further show that these fibers can be used for producing thin and transparent diamond-containing coatings with very high diamond contents. Fibers and films of polyacrylonitrile (PAN) and ND have been manufactured and characterized. To show the applicability of this method to other polymer systems, we also introduced diamond into polyamide 11 (PA 11).

RESULTS AND DISCUSSION

Air-oxidized ND powder used in this study contains both the individual particles and loosely bound agglomerates (Figure 1a,b), as indicated in ref 7. Low resolution TEM micrographs (Figure 1a,b) were recorded at a strong defocus to provide clear imaging of the particles through the appearance of Fresnel fringes and enhanced contrast. High resolution TEM (Figure 1c) revealed mostly pristine diamond particles with little content of disordered carbon. However, a variety of oxygen-containing functional groups present on the diamond surface leads to easy agglomeration of ND due to hydrogen bonding and van der Waals forces acting between the individual particles. HCl treatment of ND conducted after oxidative purification selectively increases the number of surface carboxylic groups due to hydrolysis of anhydrides, esters, lactones and other C=O containing groups formed during air oxidation, thus resulting in better suspension stability in polar solvents because of increased negative charge on the surface of the particles upon dissociation of $-\text{COOH}$.

PAN was selected as a comprehensively characterized polymer, which was previously used to manufacture pure carbon fibers, as well as silicon carbide (SiC) and carbon nanotube containing fibers by electrospinning.^{15,20,39} Representative SEM and TEM images of the ND-PAN fibers are shown in Figure 2. We usually did not observe primary particles of 5 nm in size in the electrospun nanofibers, rather we observed small agglomerates with the size smaller than the fiber diameter (Figure 2b). Pure PAN nanofibers (Figure 3) were thin (34 nm average diameter) and smooth with a few instabilities per fiber, perhaps due to not quite uniform and stable electrospinning conditions.⁴⁰ Low polymer concentration, relative to the solvent, decreases the viscosity and increases the highest obtainable loading of nanodiamond. ND-PAN fibers (10 wt %)(Figure 2a,b) show a nonuniform distribution and some agglomeration of ND in the matrix, but still they are smooth and in this respect similar to the pure PAN fibers. The average fiber diameter decreases with the increasing diamond content from 0 to 17 wt %, reaching about 15 nm. Further increases of ND content lead to larger fibers with less uniform diameters. The size and number of beads increases as the concentration of nanodiamond increases between 20 and 60 wt %. Although it is still possible to produce fibers of 60 wt % ND-PAN composite (Figure 2d), their diameter is larger and less uniform. However, while fiber diameter distribution broadens as the

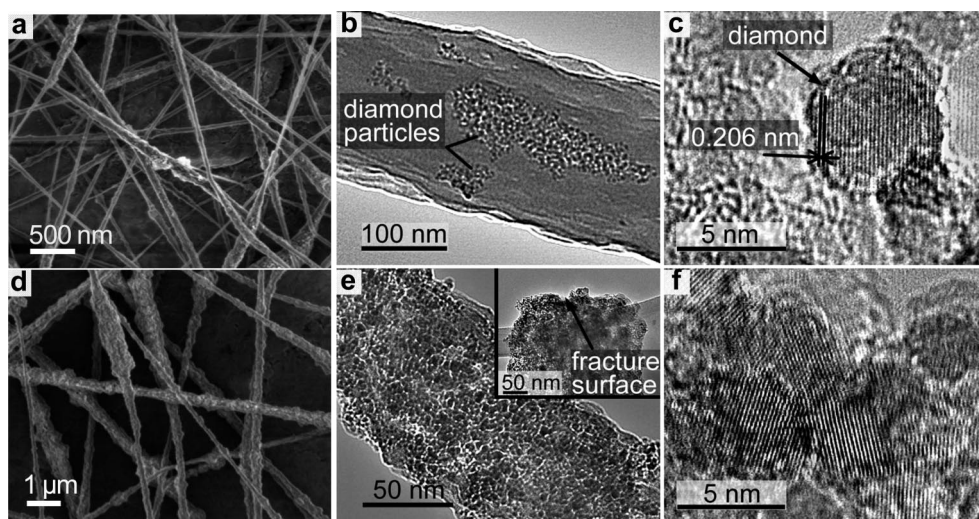


Figure 2. (Top row) SEM (a) and TEM (b,c) images of electrospun PAN nanofibers with 10 wt % ND incorporation. (Bottom row) SEM (d) and TEM (e,f) images of electrospun PAN nanofibers with 60 wt % ND incorporation. Nanodiamond particles, which have a higher density than PAN, appear as dark spots in TEM images in panels b and e. Inset in panel e shows a fracture surface of a polymer-bonded diamond fiber (60 wt % of ND in the polymer).

concentration of the ND increases above 20 wt %, the fibers appear to have a more uniform distribution of diamond particles in the polymer (compare Figure 2b and 2e). It is particularly important to notice a uniform distribution of nanodiamond throughout the fiber even at high ND loads, as seen in Figure 2e. Fast evaporation of the solvent during electrospinning suppresses re-agglomeration resulting in significantly improved nanodiamond dispersion, compared to traditional mixing techniques, and in an increased area of contact between the polymer and the nanodiamond particles. These fibers fail in a brittle manner at high diamond loads (inset in Figure 2e), with no necking or crazing, that were observed for pure PAN or CNT-containing PAN nanofibers.^{15,20} Diamond crystals were not affected by the spinning process as shown in Figure 2c,f. With an increase of the diamond content above 60 wt %, the viscosity of ND-PAN suspension increases, thus making electrospinning conditions far from optimal. However, even at high concentration (up to 80 wt %) it is still possible to produce beaded nanofibers. An attempt to electrospin a 90 wt % ND-PAN composite resulted in elec-

trospinning of droplets in which a majority of ND is agglomerated with small fibers connecting the clumps. Still, it gives an opportunity to obtain a polymer-bonded electrospayed ND coating on virtually any surface.

PAN fiber mats spun for 10 and 20 min were white or light gray and translucent, independent of the diamond content. This is due to light scattering on nanofibers, gaps between which (Figure 2a,d) are comparable to the wavelength of visible light. Heating to 200 °C makes fiber mats transparent due to fibers fusing to the surface and material uniformly spreading over the surface (the softening temperature of PAN is ~180 °C), leading to the formation of a continuous film, a process similar to that used for carbon nanotubes–polymer composites.²⁴ These films can be further heated to completely remove the polymer and leave a pure nanodiamond coating, which can provide seeds for chemical vapor deposition (CVD) of polycrystalline diamond films or be infiltrated with a different polymer (e.g., hard epoxy).

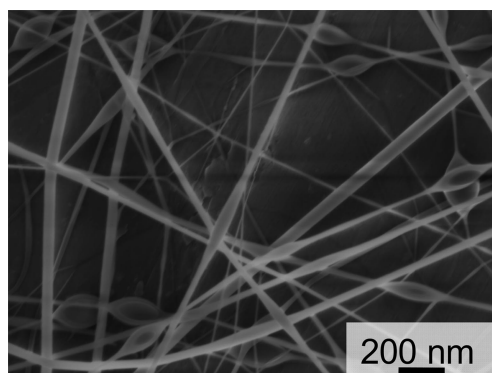


Figure 3. SEM of pure PAN nanofibers electrospun from 8 wt % PAN in DMF.

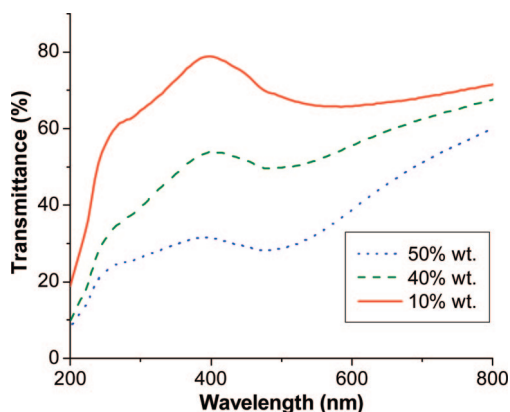


Figure 4. UV–vis spectra of the about 3 μm-thick fused PAN–ND films with different contents of nanodiamond.

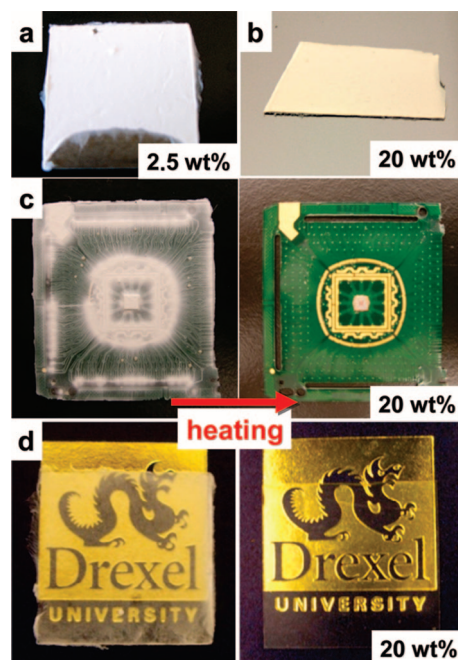


Figure 5. Optical images of electrospun PA 11 nanofibers with different loadings (wt %) of ND, on different substrates: (a) on steel, (b) on silicon, (c) on a computer chip, and (d) on a glass slide both (c,d) before (left) and after (right) heating that leads to fiber fusing to the surface and formation of a transparent film.

To study spectroscopic properties, the electrospun PAN-ND fiber mats with different concentrations of ND were heated for 20 min at 200 °C and a film of pure PAN fused *via* the same heating procedure was used as a reference in UV–vis measurements. All films used for UV–vis measurements had the same thickness of ~ 3 μm . As can be seen in Figure 4, the transmission decreases as the ND content increases from 10 to 40 wt % and finally to 50 wt %, as expected. Some absorption in the visible range may be due to about 5% of sp^2 carbon present on the surface of oxidized ND.⁷ There is a decrease of about 25% in the transmission from 10 to 40 wt % and a further decrease of $\sim 25\%$ for the 40–50 wt % samples. This shows that fairly high transparency can be maintained up to 40 wt % ND. The fact that all

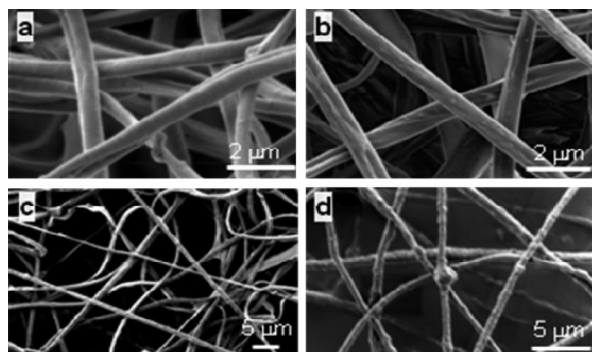


Figure 6. SEM images of PA 11 electrospun fibers with varying loads of nanodiamond: (a) 2.5 wt %, (b) 10 wt %, (c) 20 wt %, and (d) 40 wt %.

samples absorb in deep UV implies that even a small addition of nanodiamond can be used for UV protection.

We have also applied the electrospinning method to manufacture PA 11 fibers. PA 11, being produced from vegetable oil, is a nonpetroleum-based polymer. It offers the advantages of processing, a renewable resource, as well as the ability to be used as an engineering polymer with good wear resistance and chemical stability, which are important for coatings and may be further improved by diamond addition.

As-spun PA 11 fibers with various diamond contents produced a milky film on the surface (Figure 5a–c) due to light scattering. The PA 11 fibers were then fused at 180 °C for 30 min. A similar technique has been used for carbon nanotubes²⁴ and shown to preserve the distribution of the nanotubes and effectively suppress their reagglomeration. Therefore, no re-agglomeration of ND particles is expected in this process. A sample from each set was scratched with a razor blade in order to measure the film thickness using optical profilometry. The average thickness of the films spun for 20 min was 2.6 ± 0.4 μm . Similar to the PAN fibers, fused films of electrospun PA 11 fibers with ND incorporation (Figure 5c,d) show absorption in the UV range due to ND incorporation, but remain optically transparent up to at least 40 wt % of diamond. The ability to absorb UV radiation while remaining transparent in the visible range is advantageous for many applications, such as glass coating and protective layers on UV sensitive materials. Similar to the PAN fibers, as the diamond content increases so does the surface roughness of the PA 11 fibers, as seen in Figure 6 (2.5 vs 40 wt % ND). The appearance of the fibers changes from smooth to rough to droplets as the concentration of diamond changes. The observed roughness is partially dependent on the increasing viscosity of the solution due to an increase in the concentration of nanodiamond. However, addition of nanodiamond, even up to 40 wt %, does not increase viscosity as much as just a few weight percent of nanotubes,^{15,20} thus making nanodiamond an attractive filler material for high loading of polymer matrix nanofiber composites. The roughness of these fibers may be beneficial for certain applications, such as in the biomedical field, where high surface area allows for more efficient drug delivery and provides better support for cell growth. Electrospun PA 11 fibers have a larger diameter than PAN fibers and noncircular shape, as previously reported.²³ The low conductivity of PA 11 was not affected by the addition of ND (not shown), enabling its use as an insulating and protective coating on electronic devices (Figure 5c).

Load-displacement curves obtained for ND-containing PA 11 films are shown in Figure 7a. The indentation was carried out to the depth of 300 nm ($\sim 10\%$ of the coating thickness) to minimize substrate effects on the measured properties. The addition of nanodiamond has significantly improved mechanical

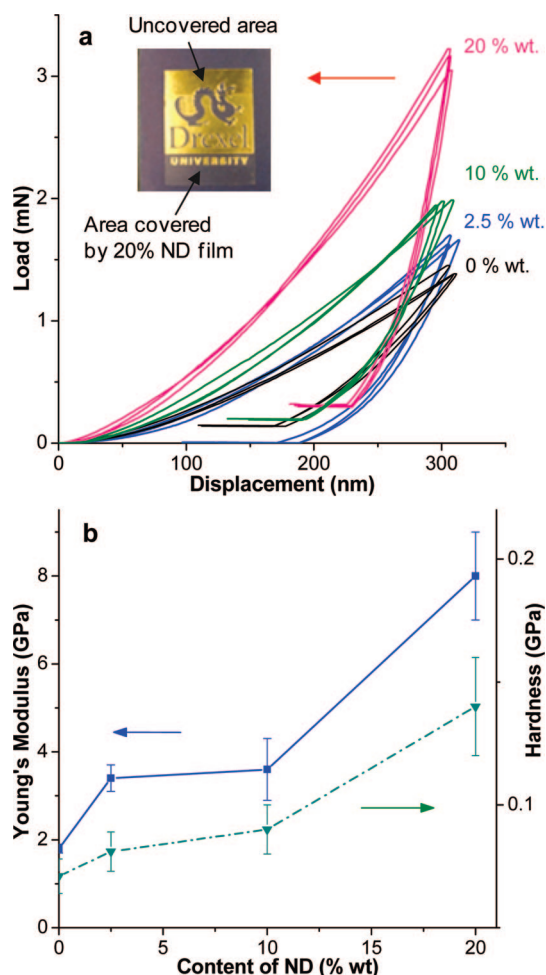


Figure 7. Load–displacement curves (a) and hardness and Young's modulus (b) of PA 11–ND films with different contents of nanodiamond. Inset in panel a shows a PA 11–ND film with 20 wt % of nanodiamond on a thin glass slide. Film thickness was $2.6 \pm 0.4 \mu\text{m}$.

properties of PA 11 films produced on Si wafer substrates, raising their Young's modulus by a factor of 4 and more than doubling the hardness, as shown in Figure 7a,b. It can be seen that if a load of 1.3 mN is required to penetrate the pure PA 11 coating to the depth of 300 nm, a 3-times higher load is required to reach the same depth for a coating with 20 wt % ND. If the scratch generated by a sharp Berkovich indenter under 5 mN load in pure PA 11 (data not shown) was $1.7 \mu\text{m}$ deep, addition of merely 10 wt % of ND led to a $0.8 \mu\text{m}$ deep scratch. Thus, scratch tests have confirmed improved hardness and scratch resistance of PA 11 after adding ND. It is important to mention that the nanoindentation and scratch tests were performed on

the films containing up to 20 wt % of ND in PA 11, since the ones with a higher content of ND showed a less smooth surface (roughness above 30 nm), which potentially may affect reproducibility of nanoindentation data. Certainly, the mechanical properties of the films can be further improved by optimization of the diamond-to-polymer ratio, better dispersion of ND in the polymer, and increasing the bonding between ND and the polymer matrix.

The results of the above study show that electrospinning is a versatile method for producing nanodiamond-containing fabrics, fibers, and coatings. The coatings were produced on a variety of substrates and there is hardly any limitation on the substrate texture or shape, as long as the material can withstand moderate heating (Figure 5, inset in Figure 7a). There is also a huge variety of polymers to choose from. In addition to PAN and PA 11, we have demonstrated incorporation of ND into bioresorbable polymers such as polyethylene oxide (PEO) and polycaprolactone (PCL), but a detailed description of those composites is outside the scope of the current paper.

CONCLUSION

Electrospun ND-containing composite nanofibers can be produced with the content of ND as high as 60–80 wt % in PAN and up to 40 wt % in PA 11. Further increases in the nanodiamond concentration, up to 90 wt % of ND in PAN, resulted in the formation of droplets rather than fibrous structures. The quality of fibers can be further improved by optimization of electrospinning process *via* incorporation of a conducting salt or further improvement of the diamond dispersion.¹² According to TEM, at 50–60 wt % of ND, the density of the nanodiamonds inside the fibers is so high that the fibers may be well-considered as ND fibers with a polymer binder.

Used as a delivery vehicle for nanodiamond coatings, electrospinning provides a quick, easy, and simple method to deposit nanodiamond with minimal agglomeration. Using thermoplastic polymers, these electrospun fibers were “ironed” onto a cotton fabric surface or fused to a flat glass, silicon, and aluminum surface yielding a thin ($3 \mu\text{m}$ or less) coating with a uniform ND distribution. Diamond-containing thin films produced by electrospinning and subsequent heating offer UV protection and improved scratch resistance to surfaces.

MATERIALS AND METHODS

Nanodiamond. The nanodiamond powder was produced *via* a detonation synthesis and supplied by Nanoblox, Inc. As-received nanodiamond powder (UD90 grade) has been thoroughly characterized elsewhere using Raman spectroscopy, TEM, XANES, and FTIR.^{7,41} Before incorporation into the polymer matrix, UD90

has been purified by air oxidation (2 h at $425 \text{ }^\circ\text{C}$) to remove non-diamond carbon and further treated in concentrated HCl at $100 \text{ }^\circ\text{C}$ for 24 h to remove metals and metal oxides by transforming them into water-soluble salts.⁷ Finally the ND powder was rinsed with DI water until reaching neutral pH. Purified ND was dispersed in a solvent that was compatible with the particular poly-

mer that is to be dissolved and then electrospun (see the following section).

Electrospinning. Two similar methods of incorporation were employed based on the matrix polymer. First, HCl treated nanodiamond was added to dimethylformamide (DMF) under stirring, sonication, and shaking. The PAN powder (purchased from Scientific Polymer Products) was then added to the suspension to produce a 6% by weight polymer solution with varying amounts of nanodiamond ranging from 0 to 90% by weight of the produced fiber. For the second polymer, PA 11 (D80 powder provided by Arkema, Inc.), the nanodiamond was dispersed in a solvent composed of formic acid (FA) and dichloromethane (DCM) in a 1:1 volume ratio. This same solvent has been previously used for electrospinning PA 11 in the concentration ranges of 1–10 wt %.^{23,24} After the ND was dispersed in FA and DCM at concentrations 2.5, 10, 20, 30, and 40% by weight of the produced fiber, the dispersions were sonicated for 1 h, and then the predissolved PA 11 was added to them and thoroughly mixed.

The electrospinning machine, a Kato Nanofiber Electrospinning Unit (NEU), was supplied by NanoBlox, Inc. The electrospinning has been performed using a horizontal and slightly inverted setup (between 0 and 45°). The unit was operated at ~23 kV for the PAN solution and between 15 and 20 kV for the PA 11 solution. A spinning distance between the syringe needle tip and the collection plate was maintained at 15 cm and the dispersions were pumped through the syringe at 0.015 cm/min in both cases. The fibers were collected on glass, aluminum foil, silicon, or TEM grids for subsequent studies.

Characterization. For UV–vis spectroscopy studies, samples of 10 wt %, 40 wt % and 50 wt % ND in PAN were electrospun onto aluminum foil covered glass slides (2 cm × 2 cm) which were rotated (180°) at the midpoint of the 20 min spinning time. The thickness of the produced fiber mats was controlled by the electrospinning time: an increased time deposits thicker fiber mats. Samples were heated to 200 °C and also left as spun for comparison purposes. Samples for nanoindentation were electrospun onto silicon wafers to achieve the maximum flatness of the surface. The nanoindentation and scratches were performed on the films containing 0, 2.5, 10, and 20 wt % of ND in PA 11 since the ones with a higher content of ND showed a less smooth surface, which may lead to large errors in the tests.

SEM analysis was performed using a Zeiss Supra 50 VP field emission SEM and a FEI XL30 environmental SEM (ESEM). TEM was performed at the University of Pennsylvania, using a JEOL 2010F operated at 100 or 200 kV. UV–vis spectroscopy was performed using a Perkin-Elmer UV–vis Lambda 35 spectrometer in reflectance mode. An optical profilometer Zygo New View 6000 was used to measure the thickness of the films. Depth sensing indentation and scratch tests were conducted at room temperature using NanoIndenter XP (MTS Corp.) equipped with a continuous stiffness measurements (CSM) attachment. The indents were performed with a spheroconical diamond indenter of 13.5 μm radius. The scratches were performed using a Berkovich tip, increasing the load linearly from 0 to 5 mN over a length of 500 μm.

Acknowledgment. The authors thank Nanoblox, Inc. for providing the nanodiamond, Arkema, Inc. for providing the PA 11, and C. Picardi of Nanoblox for helpful discussion to define the research goals. The authors also acknowledge Dr. Z. Nikolov, D. Breger, and the Centralized Research Facilities (CRF) of the College of Engineering, as well as the Chemistry Department for providing access to characterization tools, and J. Detweiler for experimental help. K. Behler, V. Mochalin, and G. Korneva were supported by an NSF Graduate Student Research Fellowship, an NTI grant through the Ben Franklin Technology Partners, and an NSF NIRT grant CTS-0609062, respectively.

REFERENCES AND NOTES

- Shenderova, O.; McGuire, G. Nanocrystalline Diamond. In *Nanomaterials Handbook*; Gogotsi, Y., Ed.; CRC Press: Boca Raton, FL, 2006; pp 203–238.
- Yushin, G. N.; Osswald, S.; Padalko, V. I.; Bogatyreva, G. P.; Gogotsi, Y. Effect of Sintering on Structure of Nanodiamond. *Diamond Relat. Mater.* **2005**, *14*, 1721–1729.
- Osswald, S.; Havel, M.; Mochalin, V.; Yushin, G.; Gogotsi, Y. Increase of Nanodiamond Crystal Size by Selective Oxidation. *Diamond Relat. Mater.* **2008**, *17*, 1122–1126.
- Portet, C.; Yushin, G.; Gogotsi, Y. Electrochemical Performance of Carbon Onions, Nanodiamonds, Carbon Black and Multiwalled Nanotubes in Electrical Double Layer Capacitors. *Carbon* **2007**, *45*, 2511–2518.
- Zhirnov, V.; Shenderova, O.; Jaeger, D.; Tyler, T.; Areshkin, D.; Brenner, D.; Hren, J. Electron Emission Properties of Detonation Nanodiamonds. *Phys. Solid State* **2004**, *46*, 657–661.
- Shenderova, O.; Petrov, I.; Walsh, J.; Grichko, V.; Grishko, V.; Tyler, T.; Cunningham, G. Modification of Detonation Nanodiamonds by Heat Treatment in Air. *Diamond Relat. Mater.* **2006**, *15*, 1799–1803.
- Osswald, S.; Yushin, G.; Mochalin, V.; Kucheyev, S. O.; Gogotsi, Y. Control of sp²/sp³ Carbon Ratio and Surface Chemistry of Nanodiamond Powders by Selective Oxidation in Air. *J. Am. Chem. Soc.* **2006**, *128*, 11635–11642.
- Mochalin, V. N.; Osswald, S.; Portet, C.; Yushin, G.; Hobson, C.; Havel, M.; Gogotsi, Y. High Temperature Functionalization and Surface Modification of Nanodiamond Powders. *Mater. Res. Soc. Symp. Proc.* **2007**, *1039*, P11.3.
- Hanada, K.; Umeda, K.; Nakayama, N.; Mayuzumi, M.; Shikata, H.; Sano, T. Characterization of Diamond Nanoclusters and Applications to Self-Lubricating Composites. *New Diamond Frontier Carbon Technol.* **2003**, *13*, 133–142.
- Shenderova, O.; Tyler, T.; Cunningham, G.; Ray, M.; Walsh, J.; Casulli, M.; Hens, S.; McGuire, G.; Kuznetsov, V.; Lipa, S. Nanodiamond and Onion-like Carbon Polymer Nanocomposites. *Diamond Relat. Mater.* **2007**, *16*, 1213–1217.
- Li, L.; Davidson, J. L.; Lukehart, C. M. Surface Functionalization of Nanodiamond Particles via Atom Transfer Radical Polymerization. *Carbon* **2006**, *44*, 2308–2315.
- Ozawa, M.; Inaguma, M.; Takahashi, M.; Kataoka, F.; Kruger, A.; Osawa, E. Preparation and Behavior of Brownish, Clear Nanodiamond Colloids. *Adv. Mater.* **2007**, *19*, 1201–1206.
- d'Almeida, J. R.; Monteiro, S. N.; Menezes, G. W.; Rodrigues, R. J. S. Diamond-epoxy composites. *J. Reinf. Plast. Compos.* **2007**, *26*, 321–330.
- Bashouti, M.; Salalha, W.; Brumer, M.; Zussman, E.; Lifshitz, E. Alignment of Colloidal CdS Nanowires Embedded in Polymer Nanofibers by Electrospinning. *ChemPhysChem* **2006**, *7*, 102–106.
- Ko, F.; Gogotsi, Y.; Ali, A.; Naguib, N.; Ye, H. H.; Yang, G. L.; Li, C.; Willis, P. Electrospinning of Continuous Carbon Nanotube-Filled Nanofiber Yarns. *Adv. Mater.* **2003**, *15*, 1161–1165.
- Li, D.; Xia, Y. Electrospinning of Nanofibers: Reinventing the Wheel. *Adv. Mater.* **2004**, *16*, 1151–1170.
- Li, D.; Wang, Y. L.; Xia, Y. N. Electrospinning of Polymeric and Ceramic Nanofibers As Uniaxially Aligned Arrays. *Nano Lett.* **2003**, *3*, 1167–1171.
- Sigmund, W.; Junhan, Y.; Hyun, P.; Maneeratana, V.; Pyrgiotakis, G.; Daga, A.; Taylor, J.; Nino, J. C. Processing and Structure Relationships in Electrospinning of Ceramic Fiber Systems. *J. Am. Ceram. Soc.* **2006**, *89*, 395–407.
- Tomczak, N.; Gu, S.; Han, M.; van Hulst, N. F.; Julius Vancso, G. Single Light Emitters in Electrospun Polymer Nanofibers: Effect of Local Confinement on Radiative Decay. *Eur. Polym. J.* **2006**, *42*, 2205–2210.
- Ye, H. H.; Lam, H.; Titchenal, N.; Gogotsi, Y.; Ko, F. Reinforcement and Rupture Behavior of Carbon Nanotubes-Polymer Nanofibers. *Appl. Phys. Lett.* **2004**, *85*, 1775–1777.

21. Yuh, J.; Perez, L.; Sigmund, W. M.; Nino, J. C. Electrospinning of Complex Oxide Nanofibers. *Phys. E* **2007**, *37*, 254–259.
22. Xiaomeng, S.; Changlu, S.; Yichun, L. Photoluminescence of Polyethylene Oxide-ZnO Composite Electrospun Fibers. *Polymer* **2007**, *48*, 1459–1463.
23. Behler, K.; Havel, M.; Gogotsi, Y. New Solvent for Polyamides and Its Application to the Electrospinning of Polyamides 11 and 12. *Polymer* **2007**, *48*, 6617–6621.
24. Havel, M.; Behler, K.; Korneva, G.; Gogotsi, Y. Transparent thin films of multiwalled carbon nanotubes self-assembled on polyamide 11 nanofibers. *Adv. Funct. Mater.* **2008**, *18*, 2322–2327.
25. Yu, S.-J.; Kang, M.-W.; Chang, H.-C.; Chen, K.-M.; Yu, Y.-C. Bright Fluorescent Nanodiamonds: No Photobleaching and Low Cytotoxicity. *J. Am. Chem. Soc.* **2005**, *127*, 17604–17605.
26. Bakowicz-Mitura, K.; Bartosz, G.; Mitura, S. Influence of Diamond Powder Particles on Human Gene Expression. *Surf. Coat. Technol.* **2007**, *201*, 6131–6135.
27. Mitura, S.; Mitura, K.; Niedzielski, P.; Louda, P.; Danilenko, V. V. Nanocrystalline Diamond, Its Synthesis, Properties and Applications. *J. Achieve. Mater. Manuf. Eng.* **2006**, *16*, 9–16.
28. Khil, M.-S.; Cha, D.-I.; Kim, H.-Y.; Kim, I.-S.; Bhattarai, N. Electrospun Nanofibrous Polyurethane Membrane as Wound Dressing. *J. Biomed. Mater. Res., B* **2003**, *67*, 675–679.
29. Kim, G. H.; Yoon, H. A Direct-Electrospinning Process by Combined Electric Field and Air-Blowing System for Nanofibrous Wound-Dressings. *Appl. Phys. A* **2008**, *90*, 389–394.
30. Li, M.; Guo, Y.; Wei, Y.; MacDiarmid, A. G.; Lelkes, P. I. Electrospinning Polyaniline-Contained Gelatin Nanofibers for Tissue Engineering Applications. *Biomaterials* **2006**, *27*, 2705–2715.
31. Rho, K. S.; Jeong, L.; Lee, G.; Seo, B.-M.; Park, Y. J.; Hong, S.-D.; Roh, S.; Cho, J. J.; Park, W. H.; Min, B.-M. Electrospinning of Collagen Nanofibers: Effects on the Behavior of Normal Human Keratinocytes and Early-Stage Wound Healing. *Biomaterials* **2006**, *27*, 1452–1461.
32. Liu, K.-K.; Chen, M.-F.; Chen, P.-Y.; Lee, T. J. F.; Cheng, C.-L.; Chang, C.-C.; Ho, Y.-P.; Chao, J. I. Alpha-Bungarotoxin Binding to Target Cell in a Developing Visual System by Carboxylated Nanodiamond. *Nanotechnology* **2008**, 205102.
33. Choi, J. S.; Leong, K. W.; Yoo, H. S. *in Vivo* Wound Healing of Diabetic Ulcers Using Electrospun Nanofibers Immobilized with Human Epidermal Growth Factor (EGF). *Biomaterials* **2008**, *29*, 587–596.
34. Huang, H.; Pierstorff, E.; Osawa, E.; Ho, D. Active Nanodiamond Hydrogels for Chemotherapeutic Delivery. *Nano Lett.* **2007**, *7*, 3305–3314.
35. Huang, H.; Pierstorff, E.; Osawa, E.; Ho, D. Protein-Mediated Assembly of Nanodiamond Hydrogels into a Biocompatible and Biofunctional Multilayer Nanofilm. *ACS Nano* **2008**, *2*, 203–212.
36. Lam, R.; Chen, M.; Pierstorff, E.; Huang, H.; Osawa, E.; Ho, D. Nanodiamond-Embedded Microfilm Devices for Localized Chemotherapeutic Elution. *ACS Nano* **2008**, *2*, 2095–2102.
37. Krueger, A.; Stegk, J.; Liang, Y.; Lu, L.; Jarre, G. Biotinylated Nanodiamond: Simple and Efficient Functionalization of Detonation Diamond. *Langmuir* **2008**, *24*, 4200–4204.
38. Chang, Y.-R.; Lee, H.-Y.; Chen, K.; Chang, C.-C.; Tsai, D.-S.; Fu, C.-C.; Lim, T.-S.; Tzeng, Y.-K.; Fang, C.-Y.; Han, C.-C.; Chang, H.-C.; Fann, W. Mass Production and Dynamic Imaging of Fluorescent Nanodiamonds. *Nat. Nano* **2008**, *3*, 284–288.
39. Ye, H.; Titchenal, N.; Gogotsi, Y.; Ko, F. SiC Nanowires Synthesized from Electrospun Nanofiber Templates. *Adv. Mater.* **2005**, *17*, 1531–1535.
40. Fong, H.; Chun, I.; Reneker, D. H. Beaded Nanofibers Formed during Electrospinning. *Polymer* **1999**, *40*, 4585–4592.
41. Osswald, S.; Gurga, A.; Kellogg, F.; Cho, K.; Yushin, G.; Gogotsi, Y. Plasma Pressure Compaction of Nanodiamond. *Diamond Relat. Mater.* **2007**, *16*, 1967–1973.